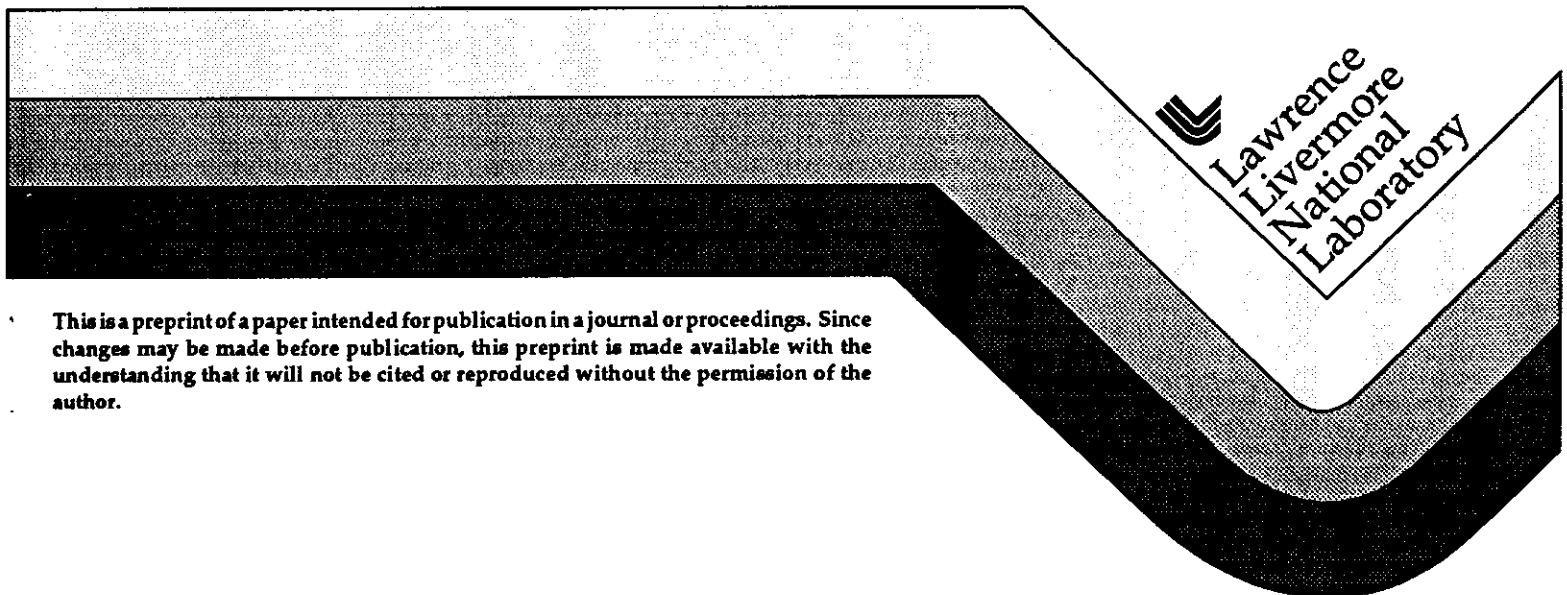


## Beam Control and Diagnostic Functions in the NIF Transport Spatial Filter

F. R. Holdener, E. Ables, E. S. Bliss,  
S. J. Boege, R. D. Boyd, C. J. Chokol,  
D. T. Davis, R. D. Demaret, R. E. English,  
C. W. Laumann, J. L. Miller, and S. W. Thomas

This paper was prepared for submittal to the  
2nd Annual International Conference on  
Solid-State Lasers for Application to ICF  
Paris, France  
October 22-25, 1996

October 22, 1996



This is a preprint of a paper intended for publication in a journal or proceedings. Since changes may be made before publication, this preprint is made available with the understanding that it will not be cited or reproduced without the permission of the author.

#### DISCLAIMER

This document was prepared as an account of work sponsored by an agency of the United States Government. Neither the United States Government nor the University of California nor any of their employees, makes any warranty, express or implied, or assumes any legal liability or responsibility for the accuracy, completeness, or usefulness of any information, apparatus, product, or process disclosed, or represents that its use would not infringe privately owned rights. Reference herein to any specific commercial product, process, or service by trade name, trademark, manufacturer, or otherwise, does not necessarily constitute or imply its endorsement, recommendation, or favoring by the United States Government or the University of California. The views and opinions of authors expressed herein do not necessarily state or reflect those of the United States Government or the University of California, and shall not be used for advertising or product endorsement purposes.

## Beam control and diagnostic functions in the NIF transport spatial filter

Fred R. Holdener, Elden Ables, Erlan S. Bliss, Steve J. Boege, Robert D. Boyd,  
Clifford J. Choccol, Donald T. Davis, Robert D. Demaret, R. Ed English,  
Curt W. Laumann, John L. Miller and Stanley W. Thomas

Lawrence Livermore National Laboratory, Livermore, CA 94550

### ABSTRACT

Beam control and diagnostic systems are required to align the National Ignition Facility (NIF) laser prior to a shot as well as to provide diagnostics on 192 beam lines at shot time. A design that allows each beam's large spatial filter lenses to also serve as objective lenses for beam control and diagnostic sensor packages helps to accomplish the task at a reasonable cost. However, this approach also causes a high concentration of small optics near the pinhole plane of the transport spatial filter (TSF) at the output of each beam. This paper describes the optomechanical design in and near the central vacuum vessel of the TSF.

(Keywords: control, diagnostic, laser, pinhole, spatial filter, reticles, wavefront, centroids, target)

### 2. INTRODUCTION

The NIF will be capable of delivering 1.8MJ of energy to target with a peak power of 500TW at a wavelength of  $0.351\mu\text{m}$  ( $3\omega$ ). Diagnostic instruments must measure beam energy, power versus time, wavefront quality, and transverse intensity profile while alignment systems must assure that the beam passes through the system correctly and is delivered accurately to the target. Many of these functions are implemented in or near the TSF, which must also accommodate components associated with propagation of the main beam through the system. Figure 1 shows the NIF laser facility and the location of the TSF.

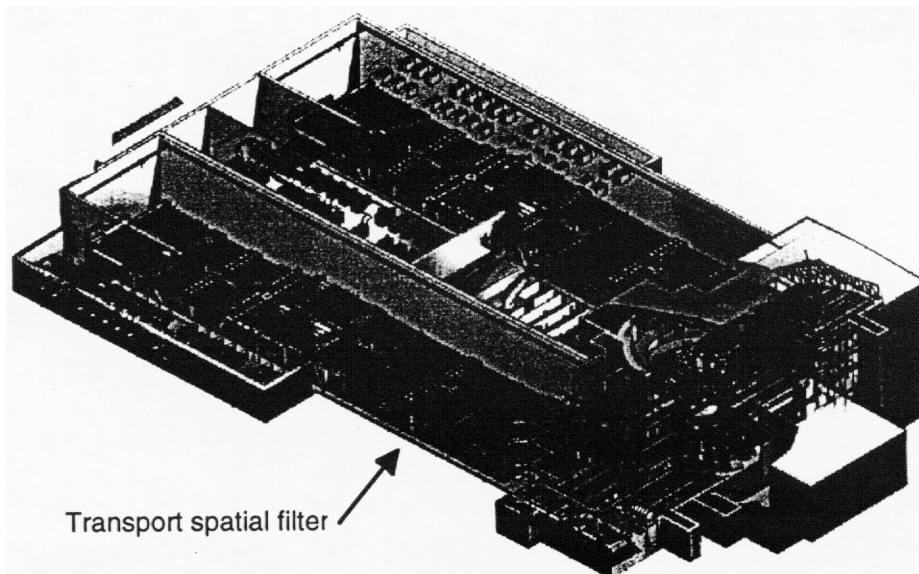


Fig. 1. NIF laser facility showing location of TSF

Figure 2 is an isometric simplified view of the beam path. A 45 mm square beam formed in the pre-amplifier module (PAM) propagates via the preamplifier beam transport system (PABTS) to the TSF injection mirror. The injected beam must match the  $f/80.7$  of the TSF as well as project an image of the input apodizer (relay plane) 16.8 m past SF3. Congestion in the vicinity of the TSF pinholes strongly influences the design of the injection optics. A compact telephoto design for the injection telescope, using spherical fused-silica elements, provides an effective focal length of 3.6 m, with a back focal length of 1.2 m. Wavefront performance is diffraction limited over a field of view of  $\pm 1$  mrad.

After injection through pinhole #1, the beam passes through the booster amplifier, is reflected down by LM3, and reflected off of the polarizer. It passes through the cavity spatial filter (CSF) pinhole #1 and through the main 11-slab flashlamp pumped amplifier. After reflection off the deformable mirror (LM1) it passes back through the main amplifier, through pinhole #2, and is switched to vertical polarization as it passes through the activated Pockels cell. The beam can now pass through the polarizer and is reflected from mirror LM2. As it returns through the polarizer and the Pockels cell, which is still active, the beam's polarization is rotated again. It passes through pinhole #3, makes a third pass through the main amplifier, reflects a second time off of LM1, and makes a final pass through the main amplifier and through pinhole #4 in the CSF. It then proceeds through a now deactivated Pockels cell with horizontal polarization and is deflected out of the cavity by the polarizer. Finally it reflects off of LM3 and makes a second pass through the booster amplifier. The pulse exits the laser at full energy through TSF pinhole #4 and the spatial filter output lens (SF4). Propagation to the target chamber is via a series of transport mirrors (LM4-8).

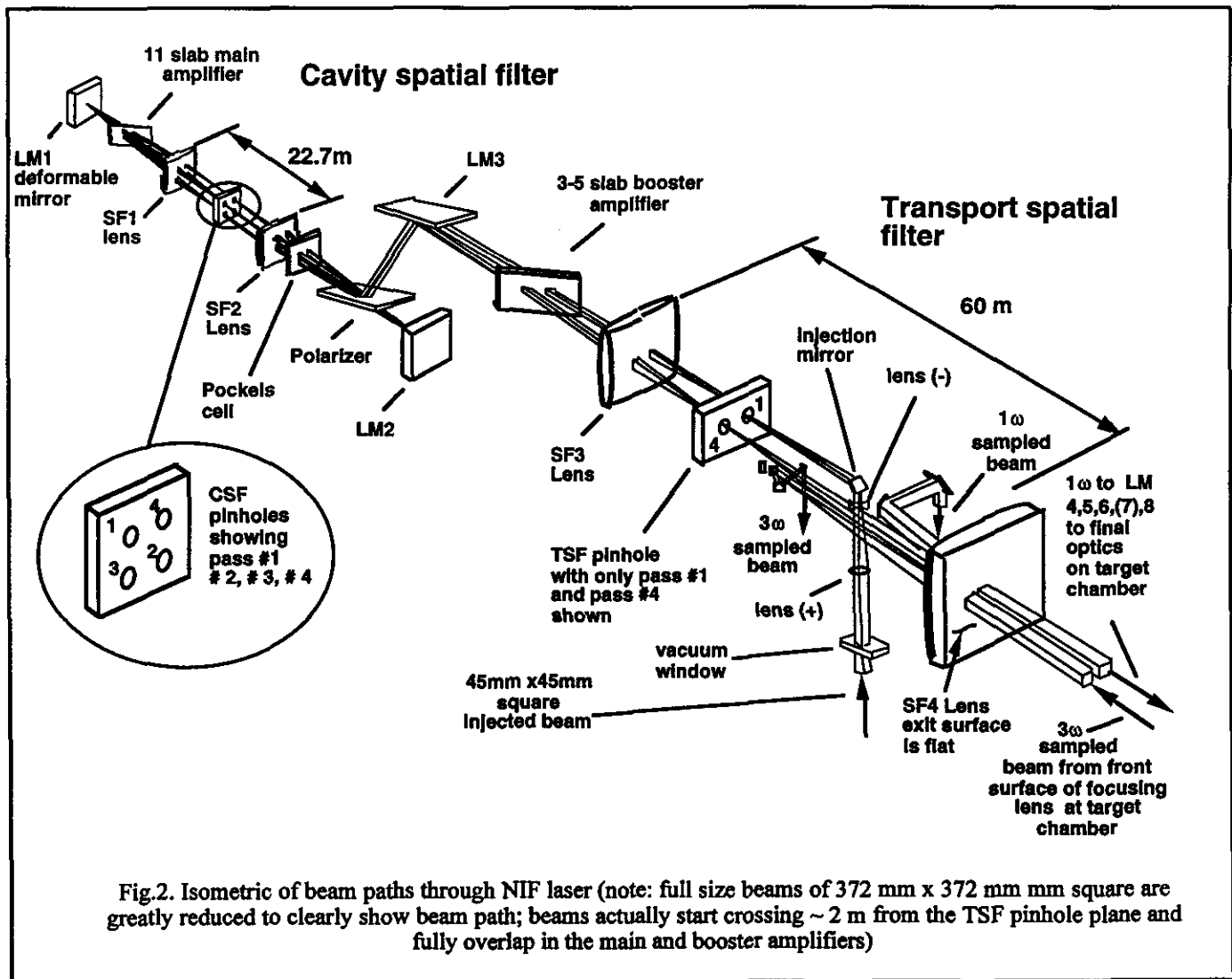


Fig.2. Isometric of beam paths through NIF laser (note: full size beams of 372 mm x 372 mm square are greatly reduced to clearly show beam path; beams actually start crossing ~ 2 m from the TSF pinhole plane and fully overlap in the main and booster amplifiers)

### 3. BEAM ALIGNMENT AND DIAGNOSTIC DESCRIPTION

To measure the properties of the beam, beam samples are taken from low reflectivity surfaces already used in the system. Figure 3 illustrates how these optical samples are handled in the central region of the TSF. The  $1\omega$  output beam is sampled at the exit surface of the TSF output lens (SF4). This surface is flat when the TSF is at vacuum, so the reflection focuses at the pinhole plane. The SF4 lens has a sol-gel AR coating with a nominal reflectivity of 0.1% and is tilted to separate the diagnostic reflection from the output beam on pass #4 in the TSF as illustrated on the right side of Figure 3. A mirror located in front of the focus picks off the beam sample. This beam sampling function determines the shape of SF4 but doesn't affect its clear aperture.

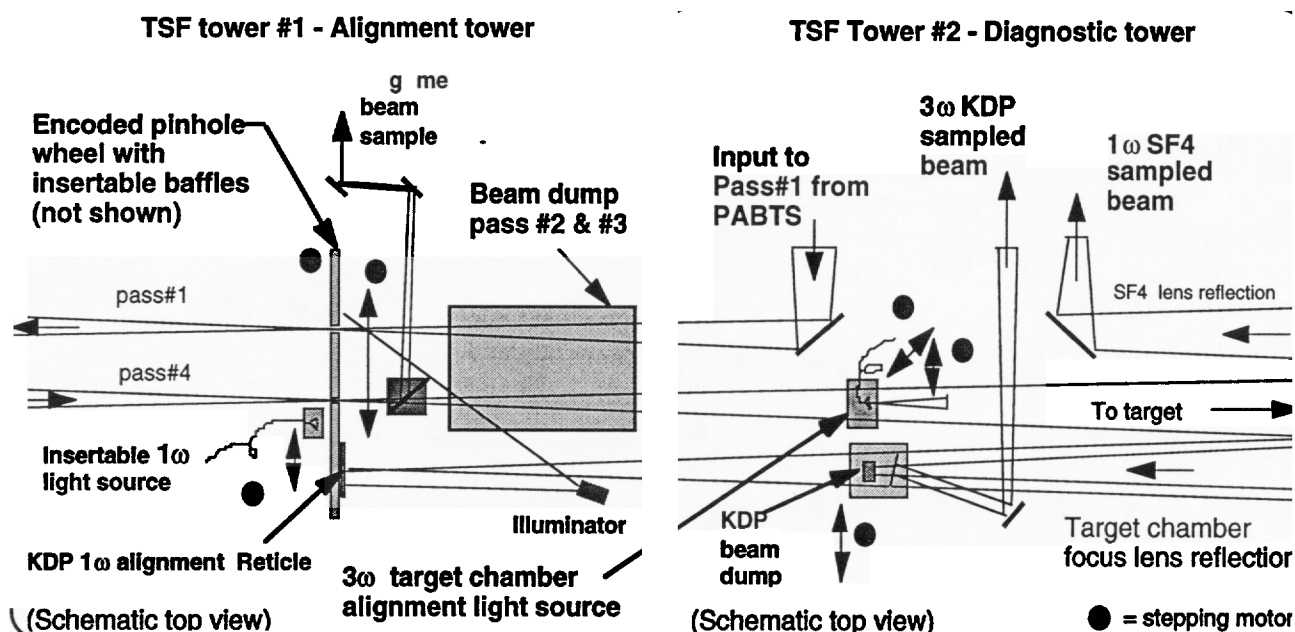


Fig. 3. Multiple functions are implemented in the region of the TSF spatial filter pinholes

The first surface of the target chamber focus lens is also flat and coated with sol-gel. It provides a  $3\omega$  beam sample that returns to the TSF by reflecting off of the transport mirrors. The maximum transmission through this set of optics is about 10% (the product of the  $3\omega$  reflectivities). The target chamber lens is also tilted to offset the reflected diagnostic beam in the TSF. This decenters the  $3\omega$  beam at SF4, and transporting the full  $3\omega$  diagnostic beam requires increasing the clear apertures of SF4 and some of the transport mirrors. The  $3\omega$  focus of SF4 is about 1.7 m in front of the  $1\omega$  focus. A remotely insertable pickoff mirror intercepts this  $3\omega$  sample and sends it to the output sensor during a shot. However, during alignment, the  $1\omega$  reflection from the target chamber lens provides a way to set the angle of the KDP frequency conversion crystals given that they are mounted referenced to one another in the final optics assembly. During KDP angle adjustment, the  $3\omega$  pickoff mirror moves out of the beam.

The diagnostic samples described above and an alignment sample from the alignment tower are transported from the TSF towers to the output sensor below the TSF as shown in Figure 4. The path lengths to the sensors are 8 to 10 meters. Each output sensor is shared between two beams using beamsplitters and shutters in the transport paths. One must choose which of the two beams to record for some diagnostics measurements on a shot, but alignment and wavefront functions are performed on both beams by temporal multiplexing during alignment.

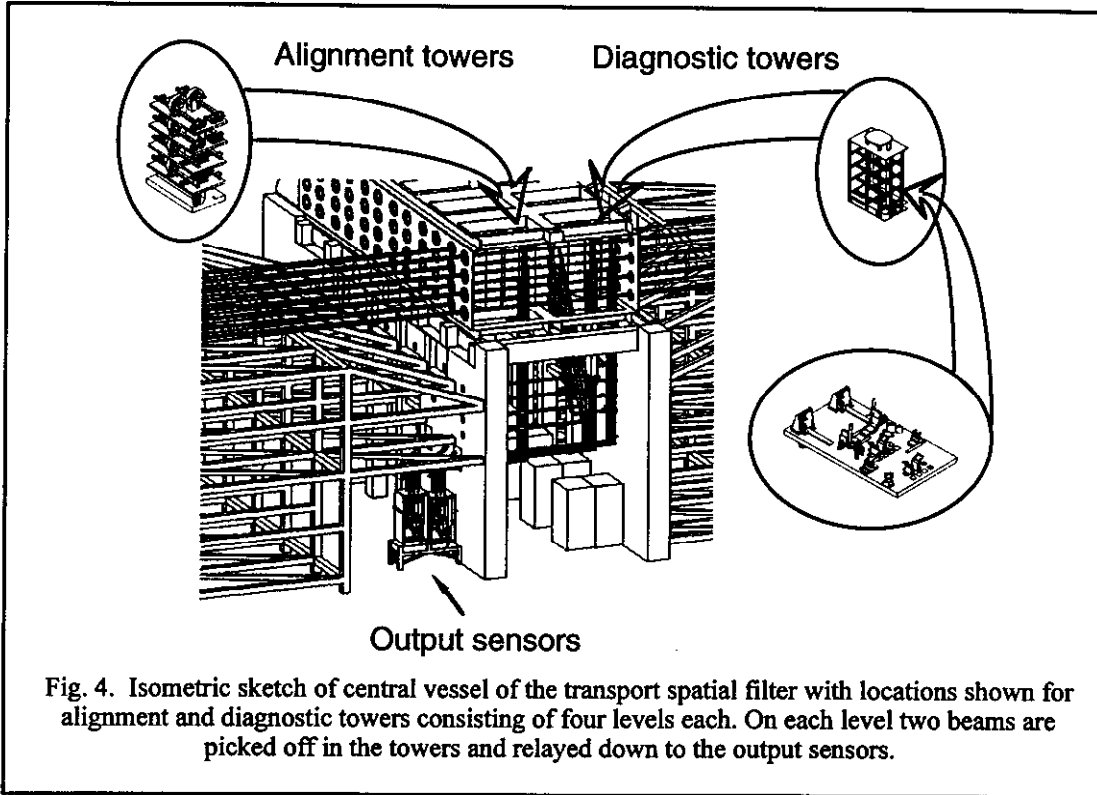


Fig. 4. Isometric sketch of central vessel of the transport spatial filter with locations shown for alignment and diagnostic towers consisting of four levels each. On each level two beams are picked off in the towers and relayed down to the output sensors.

The alignment path from the spatial filter to the output sensor delivers light for multiple functions. Figure 5 illustrates how a moving pickoff in the spatial filter determines which of five alignment functions are active: (1&2) near-field viewing of beams from passes 1 and 4 to image centering sources in the laser cavity and at the final optics; (3) far-field viewing of the pass #4 beam to monitor its output pointing; (4) far-field viewing of light scattered from a reticle at pass #1 to set the injection pointing; and finally (5) far-field viewing of the  $1\omega$  beam reflected from the final optics assembly back to a TSF reticle to set the KDP angle. The required field of view for the far-field functions is  $\pm 250 \mu\text{rad}$ , set by the angular extent of the spot reflected from the final optics and the KDP tuning range. In the near-field, the transport optics relay a 20-mm-high image of LM1 to the output sensor.

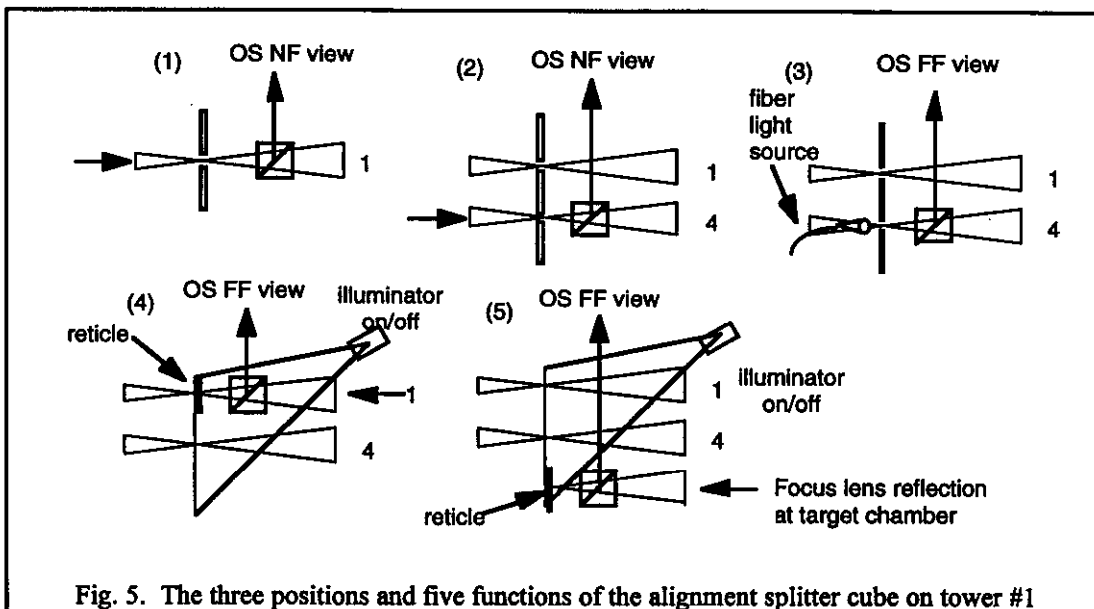


Fig. 5. The three positions and five functions of the alignment splitter cube on tower #1

The  $1\omega$  diagnostic path to the OS must have high transmission for wavefront sensor calibration, but for shots most of the energy must be dumped. Therefore the pick-off mirror is a maximum reflector and a low-transmission, partial reflector is inserted as a shot attenuator. The reflection is used for the  $1\omega$  energy diagnostic, which is an integrating sphere with a time-integrated photodiode. This is located before the merge as shown schematically in figure 6, so  $1\omega$  energies are measured for all beams. There are two afocal relays in each path to the output sensor. They provide a 20 mm wide near-field image at the output sensor. The design input angular range is  $\pm 400 \mu\text{rad}$ .

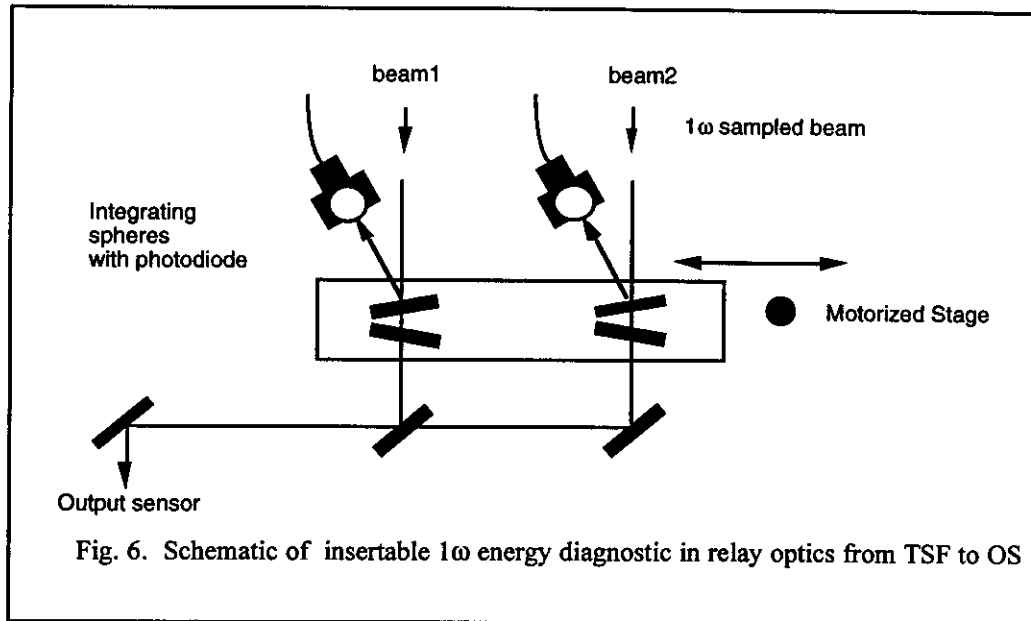


Fig. 6. Schematic of insertable  $1\omega$  energy diagnostic in relay optics from TSF to OS

For the  $3\omega$  diagnostic path high transmission is not needed. So the pick-off is an uncoated fused silica surface for maximum damage threshold. Most of the energy is dumped into an absorber behind the pick off. Two afocal relays put an image of the final optics at the OS. The design angular range is also  $\pm 400 \mu\text{rad}$ .

Six output diagnostic functions are carried out at the TSF. As described, (1) the  $1\omega$  energy is measured in the transport path, the other functions are in the OS: (2&3) Beam samples for  $1\omega$  and  $3\omega$  temporal pulse shape measurements are coupled into fiber bundles for transport to the power sensor packages<sup>1</sup>. (4&5)  $1\omega$  and  $3\omega$  near-field images are obtained using CCD cameras. (6) The  $1\omega$  wavefront (phase distribution) is measured using a Hartmann sensor comprising a lens array and CCD camera.

#### 4. DESCRIPTION OF HARDWARE NEAR THE CENTER OF THE TRANSPORT SPATIAL FILTER

In the central region of the transport spatial filter there are a pinhole holder/changer, 3 beam pickoffs, 2 reference reticles, 2 insertable fiber light sources, an incoherent light source, the main beam injection mirror/optics, and a beam dump and baffles. Use of the fiber light sources and reticles for laser and target alignment functions is described in a companion paper<sup>2</sup>. The beam dumps are for passes 2 and 3 to intercept Pockels cell leakage or back reflections from the target. These components are illustrated schematically in figure 3 with tower locations shown in figure 4. The pinhole holder/changer shown in figure 7 allows up to 10 replaceable shot pinholes, 3 alignment reticles, and an 80mm clear aperture for optics inspection.

<sup>1</sup> Thomas et. al., Temporal multiplexing for economical measurement of power versus trime on NIF, paper P27, this conference.

<sup>2</sup> Boege et. al., NIF pointing and centering systems and target alignment using a 351 nm laser source, paper 6-5, this conference.

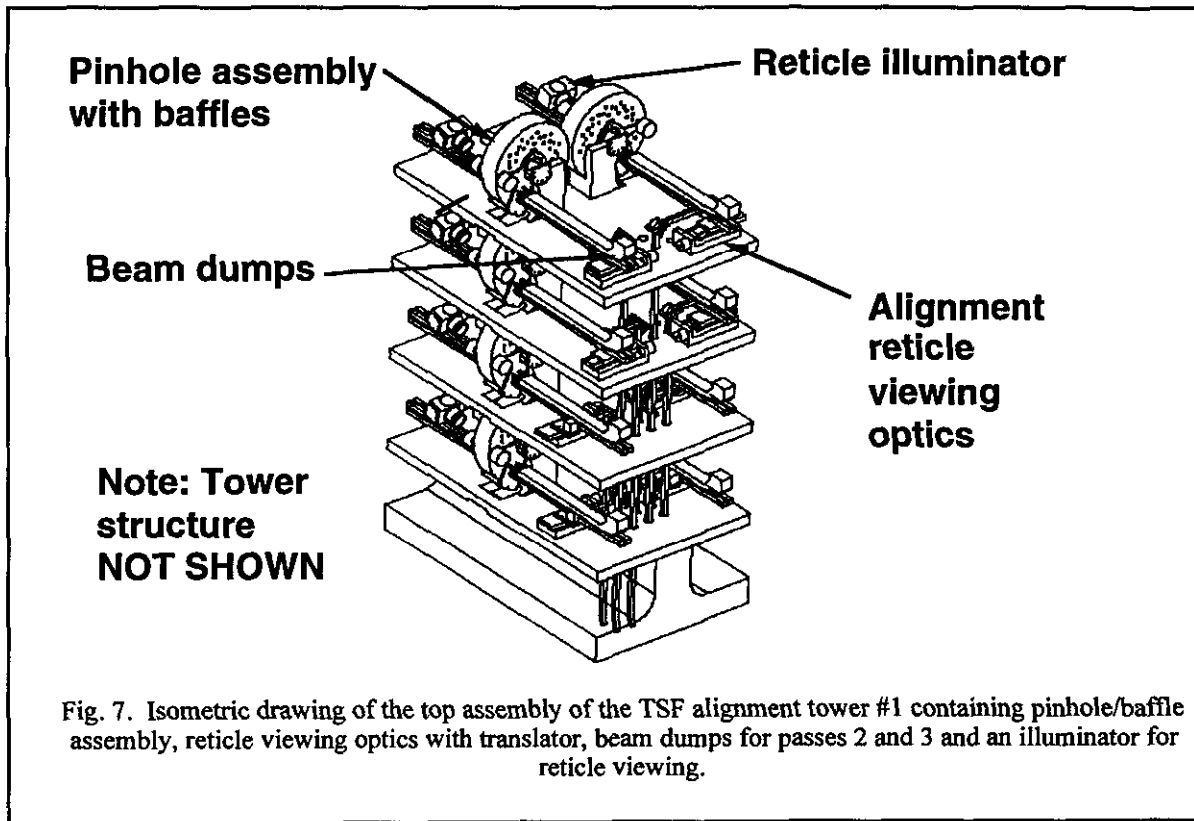


Figure 8 is a more detailed view of the pinhole/baffle assembly. On the pinhole wheel are mounted alignment reticles (pinhole #1 reticle and a focus-lens reflection reticle), an opening for optics inspection (80 mm diameter) as well as locations for 10 sets of shot pinholes. A stepping motor and metal belt drives the wheel, and a direct-coupled rotary encoder monitors its position. To achieve the required accuracy of  $5 \mu\text{m}$  repeatability, the wheel's axle rests on two precision kinematic V-blocks. A separate baffle assembly, also stepper motor driven, swings to three different locations for the four required operating modes as shown in Figure 8. For mode (1), the pass #1 reference reticle is located on axis for pointing the injected beam. A  $1\omega$  light source on the baffle assembly is positioned behind pinhole #4 for other alignment functions. In mode (2), the alignment reticles remain in place for alignment, but the baffle assembly moves the light source out of the way as part of the alignment sequence as described by Boege<sup>2</sup>. In mode (3), the large 80 mm holes in both the pinhole wheel and the baffle assembly are aligned with the normal Pass #4 beam path. This allows a clear line-of-sight through the pinhole assembly for scattered light that must be transmitted during laser optics inspection. In mode (4) the baffle and one of the ten available sets of shot pinholes are in place for a laser shot.

Figure 9 shows the complexity of the TSF diagnostic tower showing injection optics,  $1\omega$  and  $3\omega$  pickoffs, and the  $3\omega$  target chamber fiber light source. All eight beamlines are monitored on this tower where the sample beams are picked off and reflected to the central portion of the tower where they are relayed to the output sensor as illustrated. The  $3\omega$  target alignment fiber light source is mounted on a motorized x-y stage for insertion and withdrawal from the pass #4 beam path. The  $3\omega$  light is launched 1.7 m from the focal plane of the pinhole so that it is on focus at target chamber center. It is used as part of the alignment sequence for aligning beams on target with the target alignment sensor described in a companion paper<sup>2</sup>.

<sup>2</sup> Boege et. al., NIF pointing and centering systems and target alignment using a 351 nm laser source, paper 6-5, this conference.



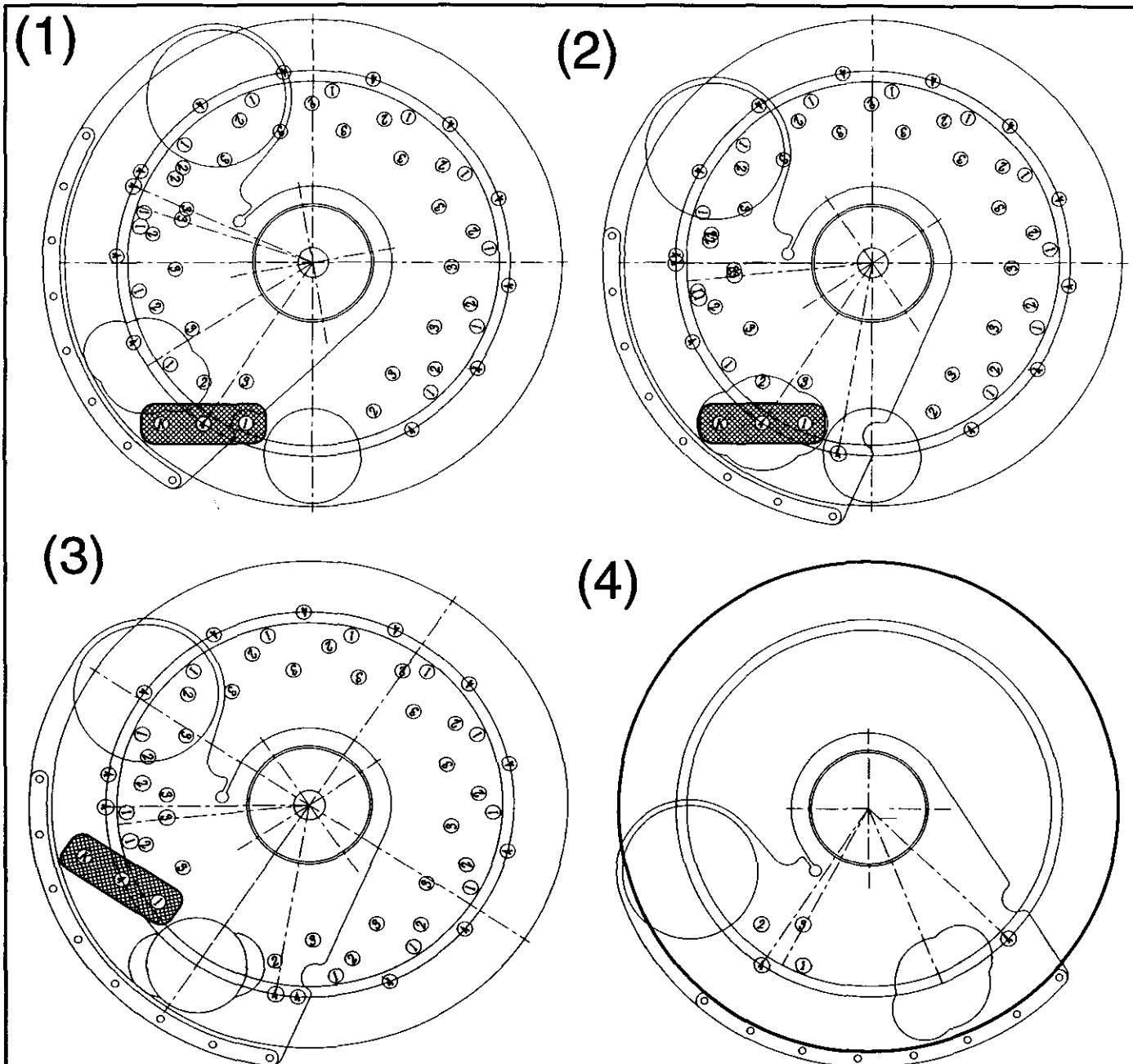


Fig. 8. Close-up of pinhole wheel with alignment reticles, 80 mm inspection open pass, and 10 sets of shot pinholes coupled with a three position baffle assembly: (1)  $1\omega$  fiber source insertable behind pinhole #4 ( $7\mu\text{m}$  repeatable position accuracy); (2) open position for observing reticles without  $1\omega$  light source; (3) open position for optics inspection (4) baffle in place for shot mode.

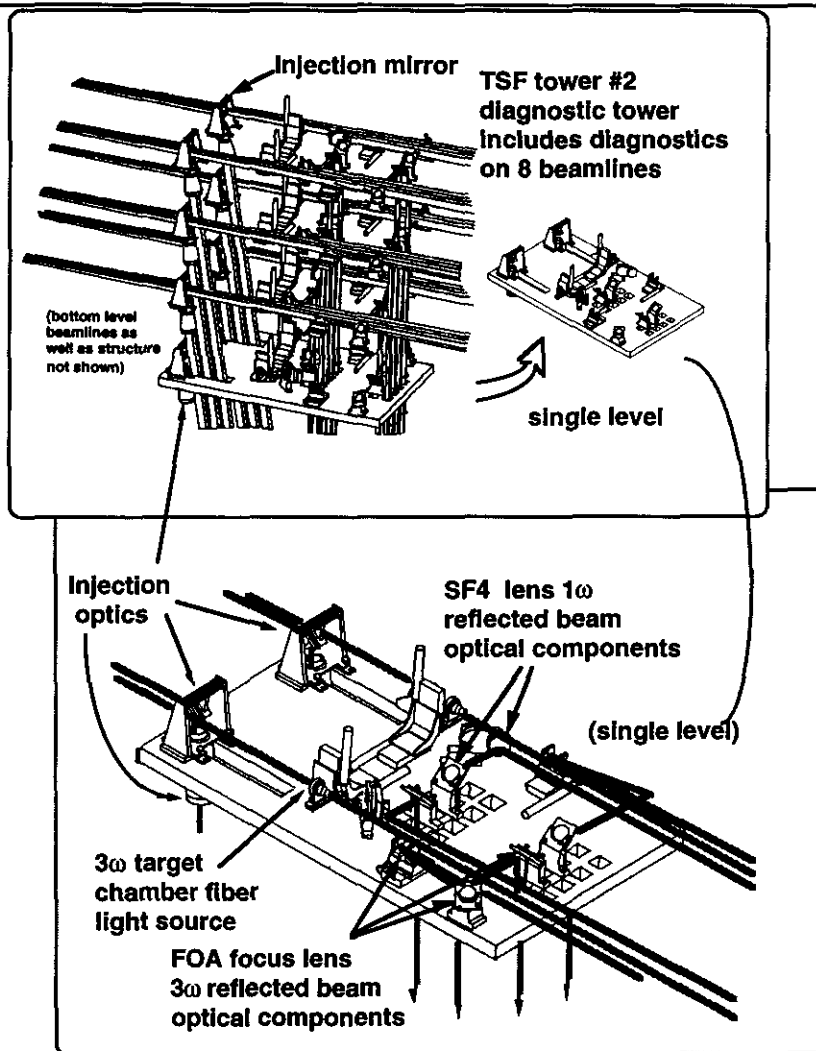


Fig. 9. TSF diagnostic tower showing injection optics and  $1\omega$  and  $3\omega$  pickoffs and  $3\omega$  target alignment fiber light source

## 5. SUMMARY

This paper has described a cost effective design for performing alignment and diagnostic functions within the TSF of the National Ignition Facility. Two sampling surfaces already part of the main laser, i.e. the exit surface of the TSF relay lens and the front surface of the final focus lens at the target chamber provide the  $1\omega$  and  $3\omega$  sample beams. These sample beams are collected in the central portion of the TSF where small optics are sufficient for implementing alignment and diagnostic functions. This concentration of components puts significant constraints on both the mechanical and optical design, but we have found the suitable preliminary design solutions.

## 5. ACKNOWLEDGMENTS

The authors wish to especially thank the design team of Jorge Victoria, Joe Lown, Paul Gschwend and Marek Kuta for their efforts in the design of these components.

This work was performed under the auspices of the U.S. Department of Energy by Lawrence Livermore National Laboratory under Contract No. W-7405-Eng-48.

*Technical Information Department • Lawrence Livermore National Laboratory*  
*University of California • Livermore, California 94551*

